



ELSEVIER

SCIENCE @ DIRECT®

PHYSICS LETTERS B

Physics Letters B 571 (2003) 132–138

[www.elsevier.com/locate/npe](http://www.elsevier.com/locate/npe)

# Measurements of anisotropic scintillation efficiency for carbon recoils in a stilbene crystal for dark matter detection

Hiroyuki Sekiya<sup>a</sup>, Makoto Minowa<sup>a</sup>, Yuki Shimizu<sup>a</sup>,  
Yoshizumi Inoue<sup>b</sup>, Wataru Suganuma<sup>a</sup>

<sup>a</sup> Department of Physics, School of Science, University of Tokyo, 7-3-1, Hongo, Bunkyo-ku, Tokyo 113-0033, Japan

<sup>b</sup> International Center for Elementary Particle Physics (ICEPP), University of Tokyo, 7-3-1, Hongo, Bunkyo-ku, Tokyo 113-0033, Japan

Received 19 March 2003; received in revised form 20 June 2003; accepted 22 July 2003

Editor: L. Montanet

## Abstract

It is known that scintillation efficiency of organic single crystals depends on the direction of nuclear recoils relative to crystallographic axes. This property could be applied to the directional WIMP dark matter detector.

The scintillation efficiency of carbon recoils in a stilbene crystal was measured for recoil energies of 30 keV to 1 MeV using neutrons from  $^7\text{Li}(p, n)^7\text{Be}$  and  $^{252}\text{Cf}$ . Anisotropic response was confirmed in low energy regions. The variation of the scintillation efficiency was about 7%, that could detect the possible dark matter signal.

© 2003 Published by Elsevier B.V. Open access under [CC BY license](https://creativecommons.org/licenses/by/4.0/).

PACS: 14.80.Ly; 29.40.Mc; 95.35.+d

Keywords: Dark Matter; WIMP; Directional detector; Organic scintillator

## 1. Introduction

It is considered that the galactic halo is composed of weakly interacting massive particles (WIMPs) as dark matter. These particles could be directly detected by measuring the nuclear recoils produced by their elastic scattering off nuclei in detectors [1]. However, nuclear recoils produced by background neutrons are indistinguishable from those by WIMPs. Therefore, one should look for statistical signature of the WIMPs. Realistic distinctive WIMP signals arise from

the earth's motion in the galactic halo. Annual modulation of event rate is one of the possible WIMP signals caused by earth's revolution around the Sun ( $\sim 30$  km/s). Actually, this signature was argued by the DAMA experiment [2].

Nevertheless, the most convincing signature of the WIMPs appears in the directions of nuclear recoils. It is provided by the earth's velocity through the galactic halo ( $\sim 230$  km/s). Assuming the WIMP halo is an isothermal sphere, the strong WIMP wind is blowing on the earth and the distribution of the nuclear recoil direction shows a large asymmetry. Hence, detectors sensitive to the direction of the recoil nucleus

*E-mail address:* [sekiya@icepp.s.u-tokyo.ac.jp](mailto:sekiya@icepp.s.u-tokyo.ac.jp) (H. Sekiya).

would have a great potential to identify WIMPs, and further, to provide information on the galactic halo [3].

It is known that scintillation efficiency of organic crystals to heavy charged particles depends on the direction of the particles with respect to the crystallographic axes [4,5]. This property makes it possible to propose a WIMP detector sensitive to the recoil direction of the nucleus [6,7]. The directional scintillation efficiency to recoil protons and carbons produced by neutrons in MeV regions was reported [8], but the recoil energy given by WIMPs is much lower.

We had measured the proton recoils in a stilbene crystal for recoil energies of 300 keV to 3 MeV and shown that the efficiency depends on the direction of the recoil proton [9]. However, carbon recoils would be more effective than proton recoils in detecting WIMPs with the interesting mass region of above 10 GeV. In this Letter, we report on the anisotropic scintillation efficiency of carbon recoils in a stilbene crystal with neutrons especially in low energy regions. We also estimate the sensitivity to the WIMP wind of the stilbene crystals.

## 2. Experimental setup

The crystal lattice of stilbenes is shown in Fig. 1. Stilbene crystals form monoclinic systems and the crystallographic axes are called  $a$ ,  $b$ , and  $c$ . The axis perpendicular to  $a$ – $b$  plane is called  $c'$ . The direction of  $c'$  axis is easily discerned because stilbene crystals are cleaved along  $a$ – $b$  plane, and according to [5], the scintillation efficiency of stilbene crystals depends on the recoil angle with respect to  $c'$ . Therefore, we measured the recoil angle dependence by changing the angle of the recoil direction with respect to  $c'$  axis ( $\theta$ ) and the angle around the  $c'$  axis ( $\phi$ ,  $\phi = 0^\circ$  was determined arbitrarily).

In order to obtain high statistics and various incident neutron energy, two neutron sources,  ${}^7\text{Li}(p, n){}^7\text{Be}$  and  ${}^{252}\text{Cf}$  were employed. The  ${}^7\text{Li}(p, n){}^7\text{Be}$  source run was performed at 3.2 MV Pelletron accelerator of the Research Laboratory for Nuclear Reactors at Tokyo Institute of Technology. Pulsed proton beam interacted with a thin lithium target, and pulsed neutrons were produced by the  ${}^7\text{Li}(p, n){}^7\text{Be}$  reaction. The repetition rate of the pulsed proton beam was set at

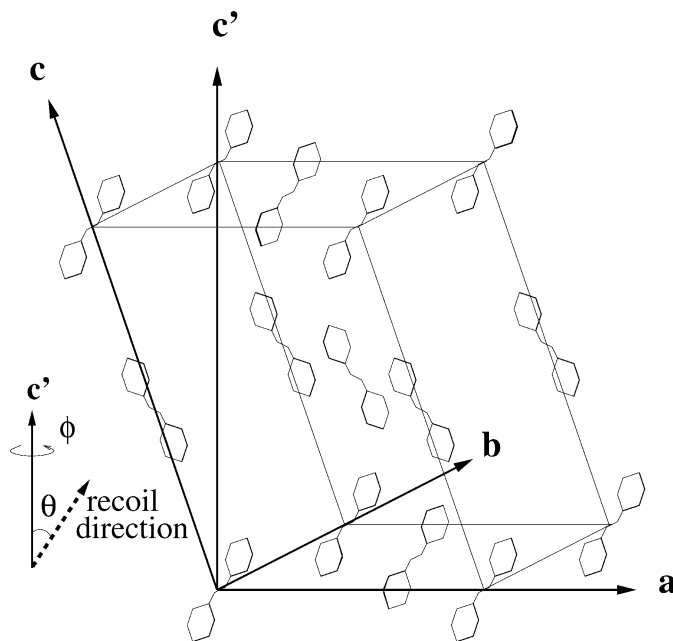


Fig. 1. Schematic drawing of the stilbene crystal lattice and the definition of the recoil angles.  $\theta$  is the recoil angle with respect to the  $c'$  axis and  $\phi$  is the angle around the  $c'$  axis.

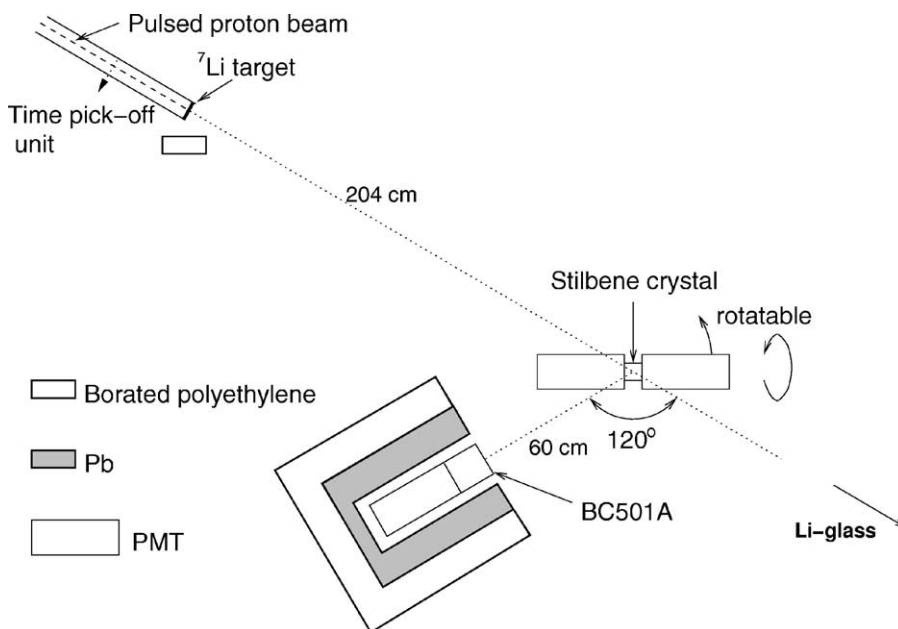


Fig. 2. Setup of the  ${}^7\text{Li}(p, n){}^7\text{Be}$  source run. Because the crystal shape is cubical and  $c'$  is perpendicular to cleavage planes where PMTs are attached, the geometrical configuration of the crystal relative to the neutron beam is same for  $\theta = 90^\circ$  and  $\theta = 0^\circ$ .

2 MHz and the pulse width was 1.5 ns. Changing proton energy three times, neutrons with energies of 200 to 650 keV were obtained. The beam and detector geometry is illustrated in Fig. 2. The temperature of the room was kept at  $26^\circ\text{C}$  during the measurement.

The dimension of the target stilbene that we measured was  $2\text{ cm} \times 2\text{ cm} \times 2\text{ cm}$ . Two opposite faces were cleaved ( $a$ - $b$  plane) and other four sides (arbitrary plane) were polished. The polished sides were covered with GORE-TEX<sup>®</sup>, and 51 mm  $\varnothing$  PMT (Hamamatsu H6411) was attached to each cleavage plane. Self-coincidence between two PMTs was required to reduce dark current events. Scattered neutron was detected by 51 mm  $\varnothing \times 51\text{ mm}$  liquid scintillator encapsulated in an aluminum cell (Saint-Gobain BC501A-MAB1) with PMT (Hamamatsu H6411). The scattering angle was fixed at  $120^\circ$  to avoid proton recoil events.

The incident and scattered neutron energies were measured by time-of-flight (TOF) method and recorded by a TDC (Hohshin C021). The coincident stilbene output was used to define the common "START". The outputs of the BC501A detector and the delayed

pulsed proton signal from the "Time Pick-off Unit" of the accelerator were used as the "STOP" signals. The PMT outputs were recorded by charge ADCs (Hohshin C009H) with two different gates—20 ns and 500 ns from the rise of the waveforms of the PMT outputs. Both stilbene and BC501A provide pulse shape discrimination (PSD) capabilities for  $n$ - $\gamma$  separation arising from the difference of the slow scintillation component fraction [4]. Consequently, the ratio of charge integrated by two different gates gives  $n$ - $\gamma$  information.

The setup of the  ${}^{252}\text{Cf}$  source run was almost the same as the  ${}^7\text{Li}(p, n){}^7\text{Be}$  source run, except the measurements of incident neutron energy. The target stilbene crystal was placed 60 cm away from the 3.5 MBq  ${}^{252}\text{Cf}$  and the BC501A detector was placed 60 cm away from the target at  $120^\circ$  of the scattering angle. To determine the timing of the nuclear fission of  ${}^{252}\text{Cf}$ , prompt gamma rays produced by the fission were detected with the 2 cm thick plastic scintillator located by the neutron source. PMT (Hamamatsu R1250) outputs were delayed and used as the "STOP" signal of the TDC.

### 3. Measurement results

The detected electron equivalent energy (visible energy) for carbon recoils in the stilbene crystal was calibrated with 5.9 keV, 6.4 keV, 14.4 keV, 22.2 keV, and 32.2 keV X/gamma rays from  $^{55}\text{Fe}$ ,  $^{57}\text{Co}$ ,  $^{109}\text{Cd}$ , and  $^{137}\text{Cs}$ . The efficiency close to the threshold was checked by the 5.9 keV X-rays. We see from Fig. 3 that the efficiency was not lost above 3 keV.

Although about 40% of neutrons interacts with the stilbene crystal more than twice in the measured energy region,<sup>1</sup> the single recoil events of neutrons scattered at  $120^\circ$  by carbons were selected using the TOFs of the incident and scattered neutrons.

However, in the  $^7\text{Li}(p, n)^7\text{Be}$  source run, there still remained background events. These were gamma ray events from  $^7\text{Li}(p, \gamma)^8\text{Be}$  (minority) and nuclear recoils in the stilbene crystal accidentally coincident with the events in the BC501A detector (majority). The gamma ray events were rejected by means of PSD of the both stilbene and BC501A detectors. The events around 0 ns of the TOF spectra of both incident neutrons and scattered neutrons are also rejected as the gamma ray events. On the other hand, to estimate the backgrounds of the accidental nuclear recoils, the measurements without requiring the coincidence of the BC501A detector were performed before and after each of the  $\theta/\phi$  run. Those background spectra were stable throughout the experiment. The stability of the beam intensity was also confirmed by the Li glass scintillator in the beam line.

The visible energy spectrum with  $\theta = 90^\circ$  for recoil energies of 100 to 105 keV is shown in Fig. 4 together with the background spectrum after gamma ray events rejection. As indicated, background spectrum was normalized and subtracted. The normalization factor was the ratio of the number of events of the higher energy regions. The shape of the background spectrum below 10 keV reflects the fact that the scintillation efficiency of proton recoils increases at low energies [10] (not the loss in efficiency near the threshold). The visible energy of that recoil energies was derived by fitting Gaussian to the spectrum above 3 keV.

The analysis procedure of the  $^{252}\text{Cf}$  source run was detailed in [9]. After the events were binned with

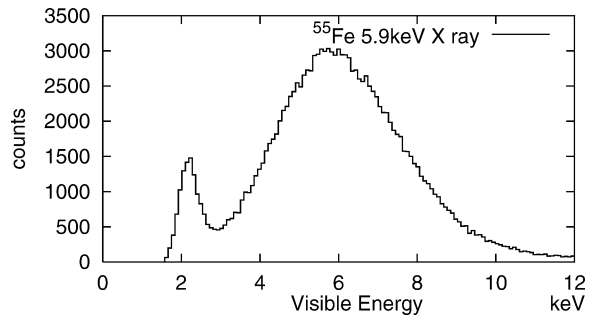


Fig. 3. The energy spectrum for 5.9 keV X-rays of  $^{55}\text{Fe}$  obtained from the stilbene crystal.

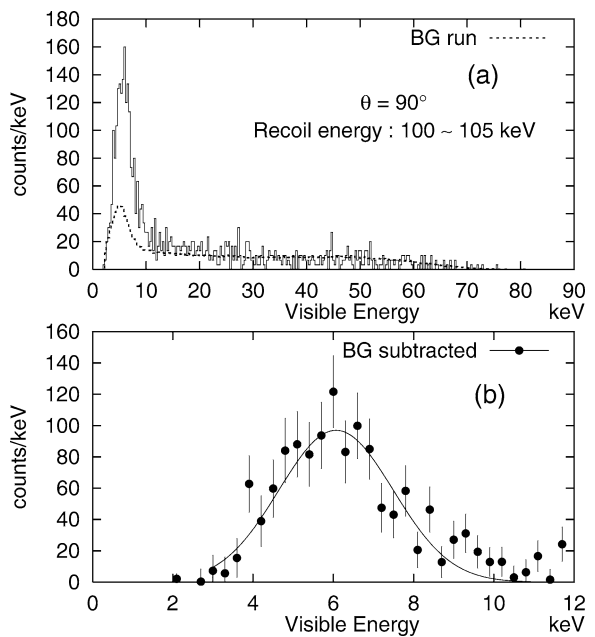


Fig. 4. (a) The visible energy spectra with  $\theta = 90^\circ$  for recoil energies of 100 to 105 keV (solid) and the normalized background (dashed). (b) The visible energy spectrum after background subtraction and the fitted Gaussian.

recoil energy, the visible energy was determined by taking the average in each bin of the recoil energy because of the small statistics.

The derived scintillation efficiency relative to the efficiency for electrons with  $\theta = 90^\circ$  and  $\theta = 0^\circ$  are shown in Fig. 5. The result is consistent with the measurements for proton recoils [9] and for charged particles in high energy regions [5], that is, the scintillation efficiency of stilbene crystal for carbon

<sup>1</sup> Based on the GEANT3 simulation.

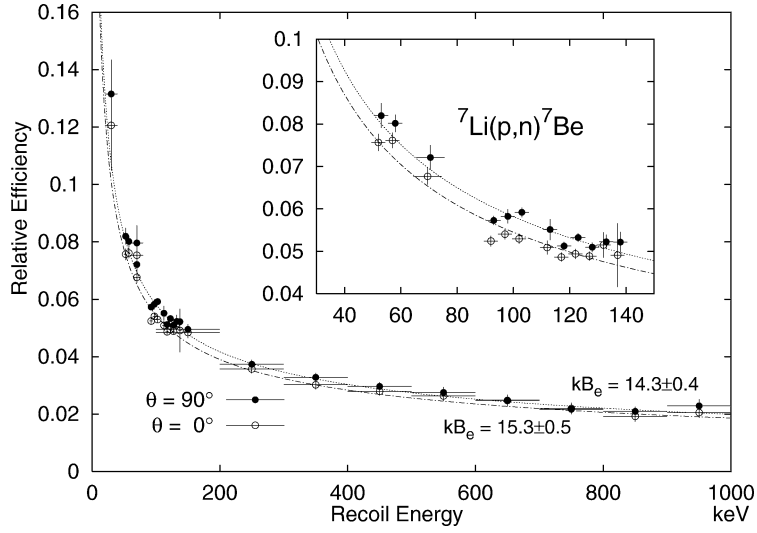


Fig. 5. The measured scintillation efficiency relative to the efficiency for electrons with  $\theta = 0^\circ$  and  $\theta = 90^\circ$  recoils ( $\phi = 0^\circ$ ). The lines show best fits to the data using Eq. (1).  $S_e/S_n$  is  $0.547 \pm 0.030$  for the both cases. The inset is the results of the  ${}^7\text{Li}(p, n){}^7\text{Be}$  source run. Horizontal error bars represent selected recoil energy region for calculating the efficiency.

recoil is maximal in the direction perpendicular to the  $c'$  axis ( $\theta = 90^\circ$ ) and minimal in the direction parallel to the  $c'$  axis ( $\theta = 0^\circ$ ). On the other hand,  $\phi$ -dependence of the scintillation efficiency was not observed in this measurement. That is also consistent with [5].

In order to estimate the response to the WIMPs, it is necessary to express the scintillation efficiency as a function of the recoil energy. The relation between the light yield ( $dL/dx$ ) and the energy loss ( $dE/dx$ ) of scintillators had been explained by Birks's empirical model [4]. However, this model does not describe the rise of the efficiency at low energies of our results. Recently, such enhancement at low energies for organic liquid scintillator was reported [10], and the light yield is introduced as

$$\frac{dL}{dx} = \frac{S_e \left(\frac{dE}{dx}\right)_e + S_n \left(\frac{dE}{dx}\right)_n}{1 + kB_e \left(\frac{dE}{dx}\right)_e + kB_n \left(\frac{dE}{dx}\right)_n} \quad (1)$$

with  $kB_e/kB_n = 3250$ . This relation is based on the assumption that electronic energy loss and nuclear energy loss contribute differently to the quenching process and scintillating process. The  $(dE/dx)$  terms are given by SRIM2003 package [11] as a function of recoil energy.

While  $S_e/S_n$ ,  $kB_e$ , or both of them could be function of the angle  $\theta$  for this experiment, it is suggested

that the response anisotropy is due to the difference in the value of the ionization quenching parameter  $kB$  [4]. Therefore, we fitted Eq. (1) to both of the measured  $\theta = 90^\circ$  and  $\theta = 0^\circ$  data at a time with the three parameters;  $kB_e(\theta = 90^\circ)$ ,  $kB_e(\theta = 0^\circ)$ , and  $S_e/S_n$ . The lines in Fig. 5 are the best fits to the data with  $kB_e(\theta = 90^\circ) = 14.3 \pm 0.4 \text{ mg/cm}^2/\text{MeV}$ ,  $kB_e(\theta = 0^\circ) = 15.3 \pm 0.5 \text{ mg/cm}^2/\text{MeV}$  and  $S_e/S_n = 0.547 \pm 0.030$  ( $\chi^2 = 68.7$ , d.o.f. = 43). Although statistics is not very high, anisotropy of 7% is seen over the measured energy region.

#### 4. Discussion

The WIMP signal by the stilbene scintillator can be obtained by comparing the visible energy spectra measured for different orientation with respect to earth's motion in the galactic halo. The variation amplitude (difference of the spectra) should be independent of any terrestrial backgrounds. Assuming spherical isothermal halo model, we estimate the expected variation of the visible energy spectrum. The differential angular rate of WIMPs in detectors with respect to laboratory recoil angle  $\gamma$  and recoil energy  $E_R$  with WIMP mass  $M_\chi$  and target nucleus mass  $M_n$  is given

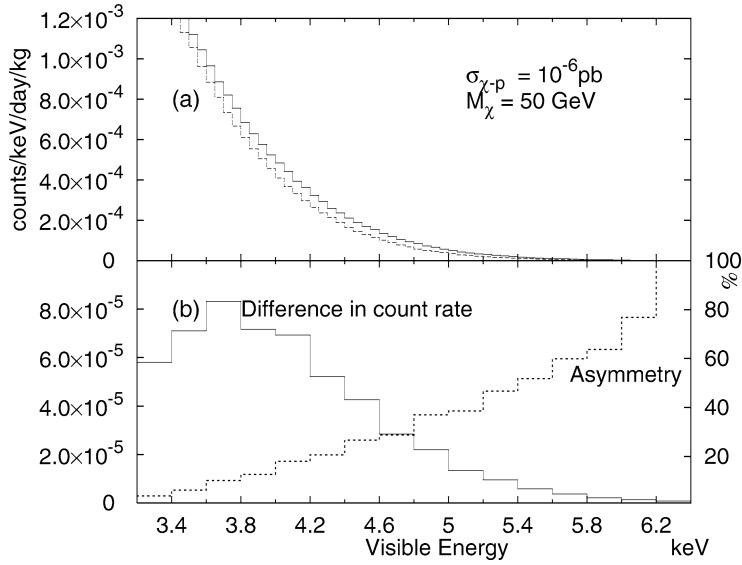


Fig. 6. (a) The expected energy spectra of the stilbene scintillator when  $c'$  axis maintained to the direction of galactic center (solid) and galactic rotation (dashed). The parameters that we used in the calculation were  $\rho_0 = 0.3 \text{ GeV/cm}^3$ ,  $v_0 = 220 \text{ km/sec}$ ,  $v_E = 232 \text{ km/s}$ , WIMP-proton spin independent cross section  $\sigma_{\chi-p} = 10^{-6} \text{ pb}$ , and  $M_\chi = 50 \text{ GeV}$ . (b) Difference in count rates and the asymmetry (= difference/average). The experimental resolution is not taken into account in the plots.

by [12]:

$$\frac{d^2R}{dE_R d\cos\gamma} = \frac{\sigma\rho_0(M_\chi + M_n)^2}{2\pi^{\frac{1}{2}}M_\chi^3M_nv_0} \times \exp\left[-\frac{(v_E\cos\gamma - v_{\min})^2}{v_0^2}\right], \quad (2)$$

where  $\rho_0$  is the local WIMP density,  $v_0$  is the velocity dispersion of the isothermal halo, and  $v_E$  is the component of the earth's velocity parallel to the galactic rotation;  $v_{\min}^2 = (M_\chi + M_n)^2 E_R / 2M_\chi^2 M_n$  is the minimum WIMP velocity that can produce  $E_R$  and  $\sigma$  is the WIMP-nucleus cross section.

We calculate by Monte Carlo method in two cases,  $c'$  axis maintained to the direction of the galactic rotation (the direction of the constellation Cygnus) and to the galactic center (the direction of the constellation Sagittarius).  $\theta$ -dependence of  $(dL/dx)$  is assumed to be trigonometric as observed in high energy region [5]. The expected spectra and the variation amplitude is shown in Fig. 6. This implies that it is plausible to use stilbene crystals for WIMP search. The variation of the spectra is much the same as that of annual modulation. However, less systematic uncertainty of the mea-

surements can be achieved because the direction of the crystal axis to the WIMP wind can be controlled.

Other organic crystals, such as anthracene and naphthalene show stronger dependence of scintillation efficiency on direction to crystallographic axis [13]. These crystals should be more sensitive to WIMP wind and the variation of the spectra should be larger. Especially, it was reported that the variation of the scintillation efficiency of naphthalene crystal is about 50%. With these organic crystals, it would also be possible to obtain some information on the motion of the galactic halo.

## 5. Conclusion

We measured the scintillation efficiency of carbon recoils in a stilbene crystal. The efficiency was observed to increase at low energies and depend on the recoil direction with respect to the  $c'$  axis. The variation of the directional anisotropy is about 7%. Assuming this anisotropic response, we estimated the sensitivity to the WIMPs and found that stilbene scintillator could detect robust WIMP signal arising from the

earth's rotation around the galactic center as compared with the annual modulation.

### Acknowledgement

We would like to thank Professor Masayuki Igashira and other members of the Research Laboratory for Nuclear Reactors at Tokyo Institute of Technology for allowing us to use the accelerator and their excellent operation.

### References

- [1] G. Jungman, M. Kamionkowski, K. Griest, *Phys. Rep.* 267 (1996) 195.
- [2] R. Bernabei, et al., *Phys. Lett. B* 424 (1998) 195.
- [3] C.J. Copi, L.M. Krauss, *Phys. Rev. D* 63 (2001) 043507; P. Gondolo, *Phys. Rev. D* 66 (2002) 103513.
- [4] J.B. Birks, *The Theory and Practice of Scintillation Counting*, Pergamon, Elmsford, NY, 1964.
- [5] P.H. Heckmann, H. Hansen, A. Flammersfeld, *Z. Phys.* 162 (1961) 84.
- [6] P. Belli, et al., *Nuovo Cimento C* 15 (1992) 475.
- [7] N.J.C. Spooner, et al., *International Workshop on Identification of Dark Matter*, World Scientific, Singapore, 1997, p. 481.
- [8] D.B. Oliver, G.F. Knoll, *IEEE Trans. Nucl. Sci.* NS-15 (1968) 122.
- [9] Y. Shimizu, et al., *Nucl. Instrum. Methods A* 496 (2003) 347.
- [10] J. Hong, et al., *Astropart. Phys.* 16 (2002) 333.
- [11] J.F. Ziegler, *The Stopping and Range of Ions in Matter SRIM2003*, <http://www.srim.org>.
- [12] D.N. Spergel, *Phys. Rev. D* 37 (1988) 1353.
- [13] K.F. Kienzle, A. Flammersfeld, *Z. Phys.* 165 (1961) 1.